Research Article

Evaluation of the American Approach for Detecting Plan Irregularity

V. Alecci [ID],[1] **M. De Stefano,**[1] **S. Galassi,**[1] **M. Lapi,**[2] **and M. Orlando**[2]

[1]*Department of Architecture, University of Florence, Piazza Brunelleschi 6, 50121 Florence, Italy*
[2]*Department of Civil and Environmental Engineering, University of Florence, Via di Santa Marta 3, 50139 Florence, Italy*

Correspondence should be addressed to V. Alecci; valerio.alecci@unifi.it

The European seismic code 8 (Eurocode 8) classifies buildings as planwise regular according to four criteria which are mostly qualitative and a fifth one, which is based on parameters such as stiffness, eccentricity, and torsional radius, that can be only approximately defined for multistory buildings. Therefore, such plan-regularity criteria are in need of improvement. ASCE seismic code, according to a different criterion, considers plan (or "torsional") irregularity in a building when the maximum story drift, at one end of the structure, exceeds more than 1.2 times the average of the story drifts at the two ends of the structure under equivalent static analysis. Nevertheless, both the ASCE approach and the threshold value of 1.2 need to be supported by adequate background studies, based also on nonlinear seismic analysis. In this paper, a numerical analysis is carried out, by studying the seismic response of an existing R/C school building taken as the reference structure. Linear static analysis is developed by progressively shifting the centre of mass, until the ratio between the maximum lateral displacement of the floor at the level is considered and the average of the horizontal displacements at extreme positions of the floor at the same level matches and even exceeds the value of 1.2. Then, nonlinear dynamic analyses are carried out to check the corresponding level of response irregularity in terms of uneven plan distribution of deformation and displacement demands and performance parameters. The above comparison leads to check the suitability of the ASCE approach and, in particular, of the threshold value of 1.2 for identifying buildings plan irregularity.

1. Introduction

In-plan irregularity is very common in existing buildings, and it is one of the most frequent sources of severe damage during earthquakes [1]. In 1985, during the earthquake of Mexico City, 42% of damaged or collapsed structures were corner buildings. Furthermore, many buildings failed in torsion due to the asymmetric layout of masonry infills [2]. The need to define adequate provisions accounting for the torsional effect due to structural asymmetry was reconfirmed by this event [3].

During the 1970s–1980s, the equivalent static analysis represented the most common method for computing seismic loads. Such a method, applied to asymmetric structures, underestimates the actions on flexible side elements, as it does not take into account the dynamic amplification of the torsional response. For this reason, researchers suggested the introduction of a design eccentricity in order to provide a torsional moment corresponding to each story of the building. In the last decades, several studies on the design eccentricity were carried out [3–12]. Later, spatial models and modal analysis became widely used by designers. Thus, the elastic response determination of in-plan irregular buildings turned easier.

In recent years, researchers focused on the inelastic response of in-plan irregular buildings. The response of asymmetric buildings was investigated by varying several parameters like centre of mass (CM), eccentricity [13], uneven distribution of concrete strength [14, 15], torsional stiffness, and periods of vibration [16]. Furthermore, several studies were developed focusing on the application of nonlinear static analysis to in-plan irregular buildings

[17–22]. Then, an important contribution that deals with torsion issue and plan regularity of building structures is provided by Anagnostopoulos et al. [23].

This paper is focused on the evaluation of the ASCE torsional provision (ASCE Standard 7-10) [24]. The response of a case study building is investigated in order to evaluate the torsional irregularity provided by the code and the corresponding uneven distribution of inelastic demand which is detected using the nonlinear dynamic analysis method.

2. Torsional Provisions

The previous generation of seismic codes was providing design eccentricities for equivalent static analysis as follows:

$$e_d = \alpha \cdot e_0 + \beta \cdot b, \tag{1}$$

where e_d is the design eccentricity, e_0 is the distance between the centre of mass (CM) and the centre of rigidity (CR) measured orthogonally to the loading direction, b is the building dimension perpendicular to the loading direction, α is a coefficient accounting for dynamic amplification of the torsional response, and β is a coefficient accounting for aleatoric position of the CM.

In Table 1, coefficients α and β are provided according to Eurocode 8 1993 (EC8-93) [25], National Building Code of Canada 1995 (NBCC-95) [26], and ASCE Standard 7-10 (ASCE 7-10) [24], where A_x is the amplification factor provided by ASCE 7-10 (defined in the following) and e_2 is the additional eccentricity provided by EC8-93, equal to the smaller of the following values:

$$e_2 = \min \begin{cases} 0.1 \cdot (L + B) \cdot \sqrt{\dfrac{10 \cdot e_0}{L}} \leq 0.1 \cdot (L + B), \\[2ex] \dfrac{1}{2 \cdot e_0} \cdot \left[\ell_s^2 - e_0^2 - r^2 + \sqrt{\left(\ell_s^2 - e_0^2 - r^2\right)^2 + 4 \cdot e_0^2 \cdot r^2} \right], \end{cases} \tag{2}$$

where ℓ_s is the radius of gyration of the floor mass in-plan (square root of the ratio of the polar moment of inertia of the floor mass in-plan (a) with respect to the centre of mass of the floor to (b) the floor mass (b)) and r is the square root of the ratio of the torsional stiffness to the lateral stiffness in the loading direction ("torsional radius").

In current code provisions, such as Eurocode 8 2004 (EC8-04) [27] and National Building Code of Canada 2010 (NBCC-10) [28], in the case of torsional irregularity, only a 3D dynamic analysis is allowed. Even when adopting a spatial model and the CQC modal combination, the accidental eccentricity is considered accounting for the random position of CM, and the design eccentricity is computed by the following equation:

$$e_d = e_0 + \beta \cdot b. \tag{3}$$

However, criteria for assessing in-plan irregularity are still very important; indeed, it affects the choice of the method of analysis and the definition of the behaviour factor.

TABLE 1: Design eccentricity coefficients.

Analyzed elements	Flexible-side elements		Stiff-side elements	
Code	α	β	α	β
EC8-93	$1.0 + e_2/e_0$	0.05	1.0	−0.05
NBCC-95	1.5	0.10	0.5	−0.10
ASCE 7-10	1.0	$0.05 \cdot A_x$	1.0	$-0.05 \cdot A_x$

Qualitatively, in-plan irregularity is due to asymmetric distributions of mass and stiffness, but quantitatively, a definition universally shared does not exist. Eurocode 8 2004 (EC8-04) provides a list of conditions to classify a building as regular in-plan:

(i) With respect to the lateral stiffness and mass distribution, the building structure shall be approximately symmetrical in plan with respect to two orthogonal axes.

(ii) The plan configuration shall be compact, i.e., each floor shall be delimited by a polygonal convex line. If in-plan setbacks (i.e., reentrant corners or edge recesses) exist, regularity in plan may still be considered as being satisfied provided that these setbacks do not affect the floor in-plan stiffness and that for each setback, the area between the outline of the floor and a convex polygonal line enveloping the floor does not exceed 5% of the floor area.

(iii) The in-plan stiffness of the floors shall be sufficiently large in comparison with the lateral stiffness of the vertical structural elements, so that the deformation of the floor shall have a small effect on the distribution of the forces among the vertical structural elements. In this respect, the L, C, H, I, and X plan shapes should be carefully examined, notably as concerns the stiffness of the lateral branches, which should be comparable to that of the central part, in order to satisfy the rigid diaphragm condition. The application of this paragraph should be considered for the global behaviour of the building.

(iv) The slenderness $\lambda = L_{max}/L_{min}$ of the building in-plan shall not be higher than 4, where L_{max} and L_{min} are, respectively, the larger in-plan and smaller dimension of the building, measured in two orthogonal directions.

(v) At each level and for each direction of analysis, the structural eccentricity e_0 and the torsional radius r shall conform to the following conditions:

$$e_o \leq 0.30 \cdot r,$$
$$r \geq \ell_s. \tag{4}$$

The first four criteria are almost qualitative, while the fifth one, if strictly applied, is valid only for single-story buildings. For multistory buildings only, approximate definitions of the centre of stiffness and the torsional radius are possible [27]. Similarly, ASCE Standard 7-10 [24] provides a

list of conditions to detect horizontal irregularity in buildings, as follows:

(i) Torsional irregularity: it is defined to exist if the maximum story drift, computed including accidental torsion with $A_x = 1.0$, at one end of the structure transverse to an axis, is more than 1.2 times the average of the story drifts at the two ends of the structure. Torsional irregularity (equation (5)) requirements apply only to structures in which the diaphragms are rigid or semirigid:

$$\delta_{max} \geq 1.2 \cdot \delta_{avg}, \tag{5}$$

where $\delta_{avg} = (\delta_A + \delta_B)/2$ is the average deflection determined by an elastic analysis (Figure 1) and $1 < A_x = [\delta_{max}/1.2 \cdot \delta_{avg}]^2 \leq 3$ is the amplification factor of the accidental torsional moment.

(ii) Extreme torsional irregularity: it is defined to exist if the maximum story drift, computed including accidental torsion with $A_x = 1.0$, at one end of the structure transverse to an axis, is more than 1.4 times the average of the story drifts at the two ends of the structure. Extreme torsional irregularity requirements (equation (6)) apply only to structures in which the diaphragms are rigid or semirigid:

$$\delta_{max} \geq 1.4 \cdot \delta_{avg}. \tag{6}$$

(iii) Reentrant corner irregularity: it is defined to exist where both plan projections of the structure beyond a reentrant corner are greater than 15% of the plan dimension of the structure in the given direction.

(iv) Diaphragm discontinuity irregularity: it is defined to exist where there is a diaphragm with an abrupt discontinuity or variation in stiffness, including one having a cut-out or open area greater than 50% of the gross enclosed diaphragm area or a change in effective diaphragm stiffness of more than 50% from one story to the next.

(v) Out-of-plane offset irregularity: it is defined to exist where there is a discontinuity in a lateral force-resistance path, such as an out-of-plane offset of at least one of the vertical elements.

(vi) Nonparallel system irregularity: it is defined to exist where vertical lateral force-resisting elements are not parallel to the major orthogonal axes of the seismic force-resisting system.

The ASCE Code (ASCE 7-10) [24] provides a simpler approach for detecting torsional irregularity. Such a method involves directly the structural response of the building, and it does not require the knowledge of specific characteristics (that are mandatory in Eurocode 8), such as the torsional radius, that can be only approximately defined for multistory buildings. The criterion provides the implementation of a linear static analysis taking into account the accidental eccentricity ($\beta = 5\%$). As shown previously, when the
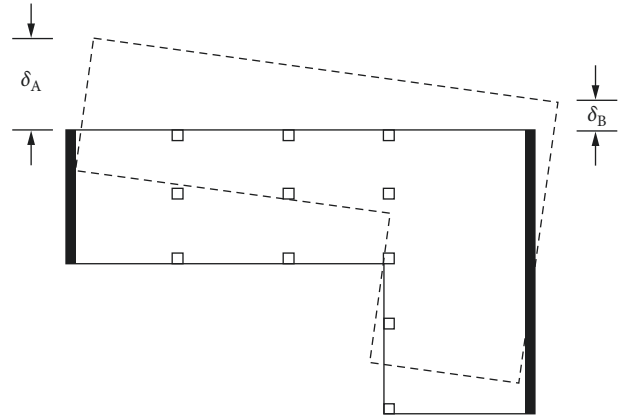

FIGURE 1: Determination of the average deflection δ_{avg}, adapted from [18].

maximum story drift is more than 1.2 times the average drift, the torsional irregularity is detected. The use of this elastic index (i.e., the ratio between the maximum and the average elastic drift) appears to be very simple and effective; however, some further researches are needed. Both the ASCE approach and the threshold value of 1.2 must be supported by adequate background studies.

With this aim, in this paper, a numerical analysis is carried out, by studying the seismic response of an existing R/C school building. As provided by ASCE 7-10, static elastic analyses are performed varying, step by step, the CM position and checking the ratio between the maximum and the average lateral displacements ($\delta_{max}/\delta_{avg}$). Lastly, nonlinear dynamic analyses are carried out in order to evaluate the corresponding level of response irregularity in terms of uneven distribution of inelastic demand.

3. Case Study

The school building under analysis is about 40 years of age, and it is situated on a flat ground in the Municipality of Prato (PO), Italy. It consists of two independent blocks: the school and the gym.

The school block has been chosen as the case study for the seismic analyses because it is made of a R/C framed structure (conversely, the gym block has a precast structure).

The school block (Figure 2) has an elongated rectangular plan, approximately 49 by 13 meters, and it is a three-story building above the ground level. The floor-to-floor height is 3.30 meters. At the ground floor, along the shorter side of the plan, there is a portico that covers the first span of the frames and that provides access to the entrance hall. After the entrance hall, a central corridor leads to the classes and offices along the two long sides of the plan. This distribution pattern is repeated, almost unchanged, at the upper floors as well. The external cladding, in precast panels, and the interior walls, which divide the classes, are made of hollow bricks and follow the frame scheme, and they also have ribbon windows outwards.

The building structure (Figure 3) is entirely made of R/C columns and beams, which form only three plane moment-

(a)   (b)   (c)
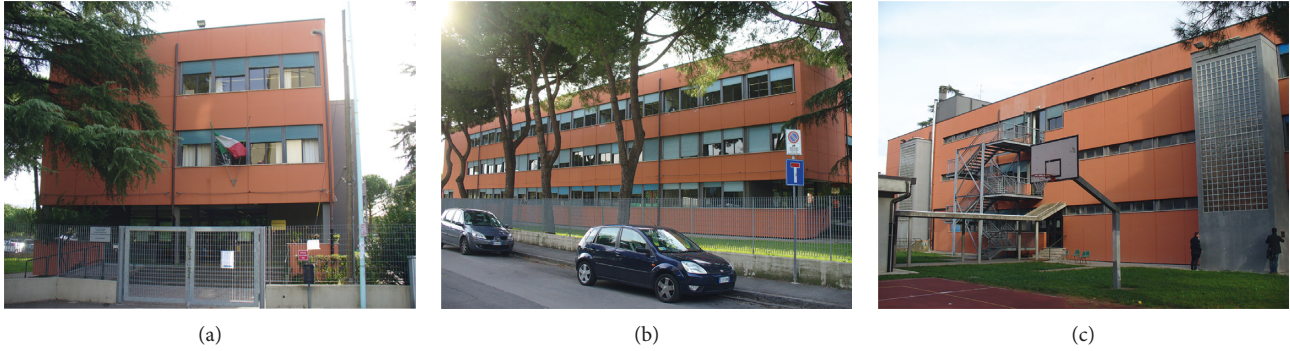
FIGURE 2: School building: (a) frontal elevation where the portico and the entrance hall are present; (b) and (c) longitudinal elevations.

resisting frames (MRF), running along the longitudinal direction. In the transversal direction, there are not MRF, excepting for the frames at the ends of the structure. The floor slabs can be considered as the rigid diaphragms.

The structural symmetry of the plan fails, in particular, at the ground floor where, due to the presence of a larger room devoted to refectory, in the central longitudinal frame, the second column is missing. Therefore, the frame beam has a span doubled and supports the column of the upper floor at midspan, and the rectangular beam cross section is 25 by 90 cm, while the others are flat beams with a cross section of 80 by 22 cm. Cross section 25 by 90 cm was also used for the corresponding beams at the two upper floors. The story floors are made of casted-in-place one-way hollow block slabs.

Instead, the rafters and the edge beams supporting the attic floor have a section of 12 by 40 cm and form a hip roof. The covering is made of insulated sandwich panels. The attic floor is not serviceable.

The columns have three different cross sections: 25 by 30 cm, 25 by 40 cm, and 25 by 55 cm. In the two longitudinal edge frames, the longer section side is arranged orthogonally to the frames, while in the central frame, the longer side follows the frame direction. In Table 2, the characteristics of the column sections at the ground floor are provided.

The concrete compressive strength was assumed to be equal to $f_c = 25$ MPa, and the steel yield stress was assumed to be $f_y = 430$ MPa.

A finite element structural model has been created, and numerical analyses have been carried out using the SAP2000 software [29]. In addition to the dead weight of the structural elements, the following loads have been considered: the weights of the story and roof floors (G_1), the permanent loads (G_2), such as the partition walls, the screed, and the tiles, and the live loads (Q). In the following, the seismic combination (7) for the ultimate limit states is provided according to the Italian Code (NTC 2018) [30]:

$$E + G_1 + G_2 + 0.6 \cdot Q, \qquad (7)$$

where E is the seismic action along the considered direction. The seismic base shear F_h has been computed in accordance with equation (8), provided by the NTC 2018:

$$F_h = S_d(T_1) \cdot \frac{W}{g} \cdot \lambda, \qquad (8)$$

where $S_d(T_1)$ is the design spectral acceleration calculated according to the fundamental period T_1 of the building (as in this case, the elastic response spectrum has been adopted, and $S_d(T_1)$ is equal to $S_e(T_1)$), T_1 is the fundamental period of the building, W is the effective seismic weight, g is the gravity acceleration, and λ factor equal to 0.85 in the case of a multistory building (with the story number greater than or equal to 3).

The elastic response spectrum $S_e(T)$ is used to calculate the seismic input for SLV verifications, assuming a building life of 50 years, and importance of class III ($C_u = 1.5$) has been obtained considering the building site (Figure 4).

In the structural model, rigid diaphragms have been considered at each building floor, so as to easily define the position centre of masses (CM).

Firstly, the model has been seismically analyzed by the equivalent static method [31], by applying the horizontal action at the CM of each story floor. The seismic force, computed according to the formulae of the Italian NTC 2018 [30], has been assumed acting in the direction of the shorter building side (y direction), where only the two edge frames exist, in order to catch the greatest displacements.

Then, nonlinear dynamic analyses have been performed using a natural earthquake accelerogram (Figure 5).

The adopted accelerogram is the record 147ya of Friuli (aftershock) earthquake happened in 1976, September 15th. The recorded magnitude (Mw) is 6, and the peak ground acceleration (PGA) is equal to 2.32 m/s².

This accelerogram was chosen because it is spectrum compatible with the adopted elastic response spectrum. In the following, a comparison between the elastic response spectrum from the Italian NTC 2018 and the 147ya spectrum is proposed (Figure 6).

To assess the seismic performance of a building, through a nonlinear dynamic analysis, the Italian NTC 2018 requires, at least, three accelerograms. Therefore, the choice of using only one accelerogram could appear inadequate. Actually, such request aims to reduce the uncertainties of the analysis, and more in general, it aims at increasing the structural safety. Since the assessment of the structural safety of the building is out of the purpose of this paper, that deals,
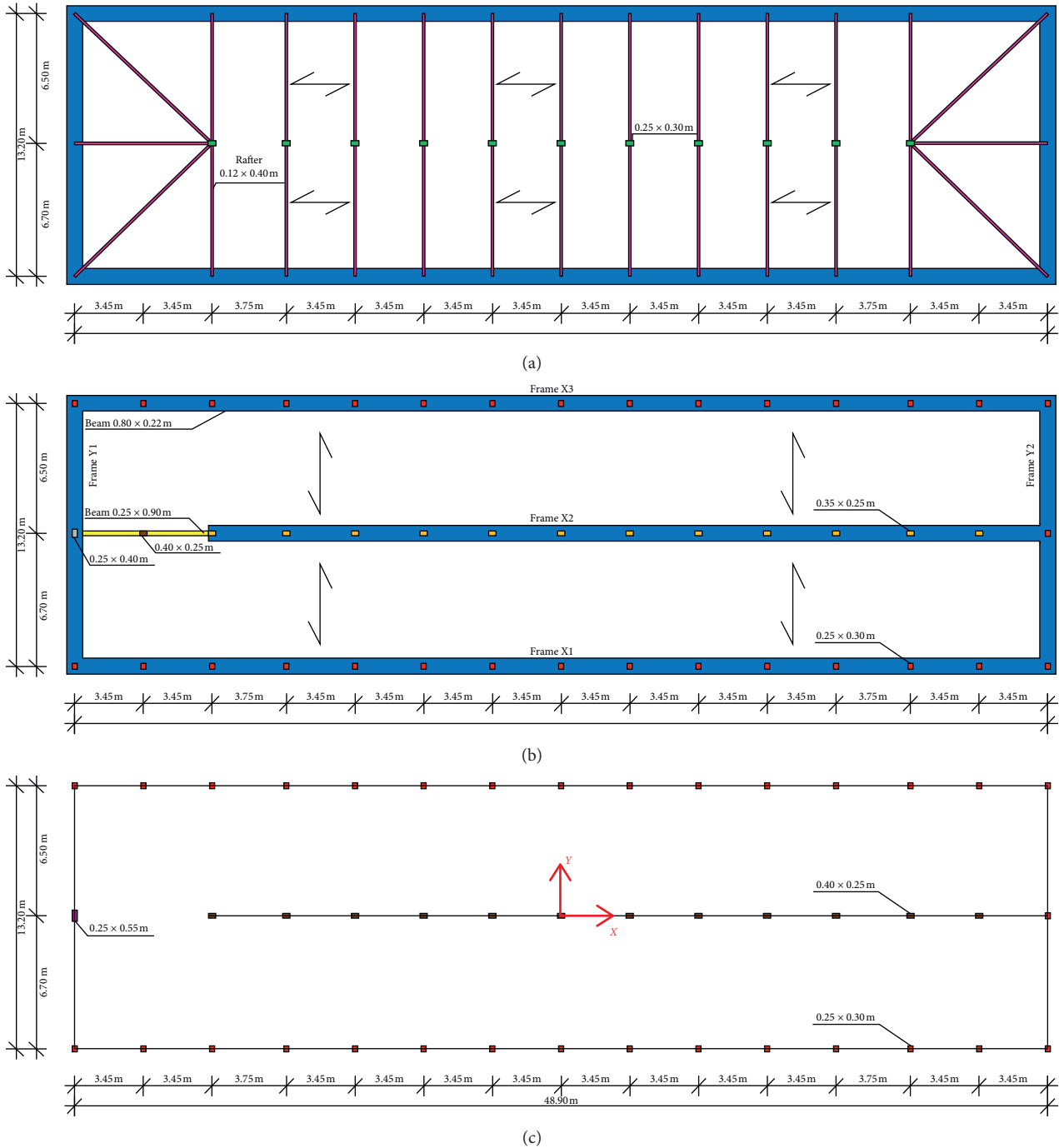
(a)

(b)

(c)

FIGURE 3: Reference plan of the building that shows the three longitudinal frames (*x* direction) and the two transversal frames (*y* direction): (a) roof plan; (b) upper floors plan; (c) ground floor plan.

instead, with the influence of the in-plan irregularity on the structural inelastic response, only one accelerogram has been considered. It is evident that also the seismic action, both in terms of intensity and frequency content, has an influence on the response of in-plan irregular buildings; however, the evaluation of this influence is out of the scope of this work.

The nonlinear dynamic analyses were conducted using lumped plasticity. In particular, at both extremities of all

TABLE 2: Characteristics of the column sections at the ground floor.

Size	Longitudinal reinforcement	Stirrups
25 × 30	4Ø16	Ø6@200
25 × 40	6Ø16	Ø6@200
25 × 55	8Ø16	Ø6@200

beams and columns, potential plastic hinges were placed. The latter were developed according to the ASCE 41-13 [32],
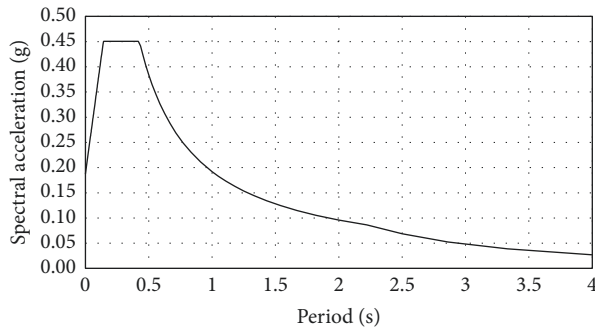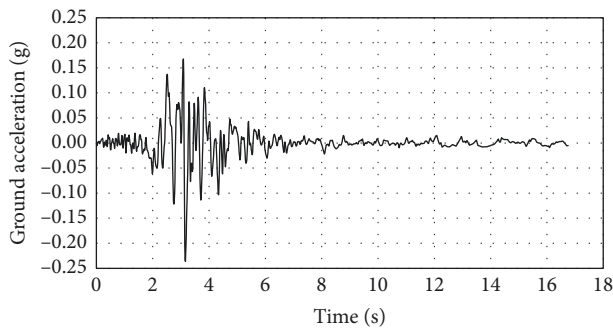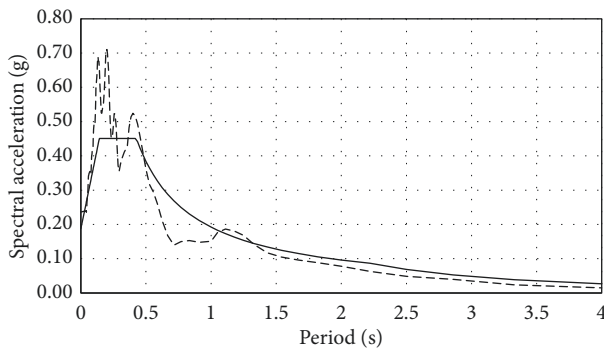
FIGURE 4: Elastic response spectrum.

FIGURE 5: Record 147ya—Friuli (aftershock), 1976, September 15th.

FIGURE 6: Comparison between the elastic response spectrum (NTC 2018) and the spectrum obtained by the record 147ya of Friuli.

and the inelastic demand (D) is expressed in terms of the plastic rotation at the chord (θ_{pl}). The capacity (C) is given by the limit life safety (LS), as defined by ASCE 41-13. In Figure 7, the idealized full backbone curve, defined according to ASCE 41-13, is shown.

The first part of the backbone curve (A-B) represents the elastic behaviour of the section, and the activation of the plastic hinge occurs beyond the point B. The peak of the strength is reached in correspondence to the point C (note that the point C does not represent the capacity), and then the strength decreases rapidly until reaching the point D where a small residual strength is still provided by the section. The failure occurs at point E where the strength drops to zero.
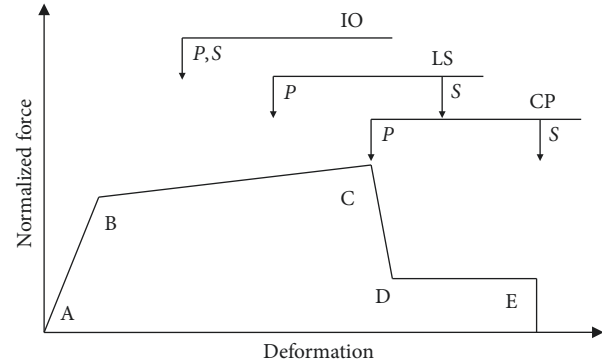

FIGURE 7: Idealized full backbone curve, acceptance criteria according to ASCE 41-13 [32].

Therefore, points A to E describe the nonlinear behaviour of the section, while the acronyms IO, LS, and CP indicate, respectively, the acceptance criteria for immediate occupancy (IO), life safety (LS), and collapse prevention (CP). For both life safety and collapse prevention, the acceptance criteria are differentiated for primary components (P) and secondary components (S). For primary components, LS = 0.75 C and CP = C but not greater than CP = 0.75 E, while for secondary components, LS = 0.75 E and CP = E.

Therefore, the capacity of the section (C) is represented by the plastic component of the LS deformation calculated as C = LS − B.

4. Results and Discussion

In this section, results of numerical analyses are presented and discussed. The gross member flexural rigidity was considered and the concrete elasticity modulus was assumed to be equal to 30 GPa.

In Table 3, the periods of vibration, the percentage of participating mass u_x along the longitudinal direction of the building (x direction), the percentage of the participating mass u_y along the transversal direction of the building (y direction), and the percentage of the mass participating to the torsional mode r_z are listed for each mode of vibration considered.

Referring to the spectral ordinate $S_d(T_1)$, associated to the fundamental period of vibration along the y direction, the static forces at each floor level are calculated. Then, equivalent static force analyses are performed in the y direction, by varying the CM position along the x direction. The same procedure is repeated for the response spectrum analysis and the ratios between the maximum and the average lateral displacements ($\delta_{max}/\delta_{avg}$), calculated with both methods at varying of the CM position, are presented in Figure 8. The effect of variation of the periods of vibration, induced by the variation of CM position, is considered negligible.

Two considerations arise from previous results. When the CM is placed in the actual position, the floor displacement includes rotational components (indeed $\delta_{max}/\delta_{avg} \neq 1$): this means that CM and CR are not aligned (CR is detected when $\delta_{max}/\delta_{avg} = 1$). The two methods, the

TABLE 3: Results of the modal analysis.

Mode	Period	u_x	u_y	r_z	$\Sigma(u_x)$	$\Sigma(u_y)$	$\Sigma(r_z)$
1	1.497	0.00	0.80	0.01	0.00	0.80	0.01
2	1.042	0.00	0.00	0.81	0.00	0.80	0.82
3	0.689	0.87	0.00	0.00	0.87	0.80	0.82
4	0.347	0.00	0.15	0.00	0.87	0.95	0.82
5	0.296	0.00	0.00	0.13	0.87	0.95	0.95
6	0.242	0.10	0.00	0.00	0.97	0.95	0.95
7	0.168	0.00	0.04	0.00	0.97	1.00	0.96
8	0.158	0.02	0.00	0.02	0.99	1.00	0.98
9	0.151	0.01	0.00	0.02	1.00	1.00	1.00

FIGURE 9: Demand to capacity ratios D/C: uneven distribution of inelastic response, CM coincident with CR.
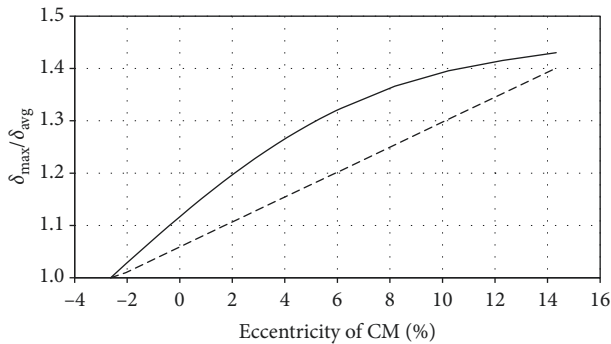

FIGURE 8: Ratios between maximum δ_{max} and average displacement δ_{avg}, at varying CM position. Comparison between linear dynamic analysis (continuous line) and linear static analysis (dotted line). The position of CM is given in % of the building longitudinal dimension ($L = 48.85$ m); for $e = 0\%$, CM is in the actual position.

equivalent static force and the response spectrum analysis, give almost the same results in term of displacements when CM is close to CR. However, increasing the distance between CM and CR, the agreement between the results gets worse, but this difference is in accordance with several researches [11, 12] and it is widely discussed in Torsional Provisions. In the present case, according to ASCE Code (ASCE 7-10) and considering the 5% of accidental eccentricity, the building resulted in regular in-plan since the ratio between maximum and average displacement resulted lower than $\delta_{max}/\delta_{avg} < 1.2$ (Figure 8).

Then nonlinear dynamic analyses are performed in order to assess the uneven distribution of inelastic response at varying CM position. In particular, four analyses are performed: the first considers CM coincident with CR, the second considers CM in its actual position, and the third and fourth consider CM in the positions that give $\delta_{max}/\delta_{avg}$ equal to 1.2 and 1.4, respectively, in the equivalent static force analysis (Figure 8).

In Figure 9, the ratios between inelastic demand D and capacity C (D/C), calculated by means of nonlinear dynamic analyses, of all columns at the ground floor, are shown in order to evaluate the damage levels. As previously said, in the y direction, the only frames are placed on the left and right side of the building. All the other columns, placed between these two frames, have to be considered as cantilever since such columns are not connected by beams in the y direction.
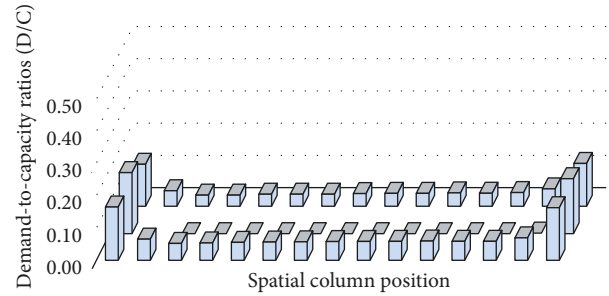
This fact explains why the columns placed on the left and right side of the building are much more affected by the inelastic demand than the others.

Furthermore, the columns placed in the centerline have the longer side of the cross section oriented along the x direction, instead the columns placed on the first and third line have the longer side of the cross section oriented along the y direction. For this reason, the inelastic demand of the centerline columns is lower than that of the columns placed on the first and third lines, due to the greater shear force brought by the latter. Although the uneven distribution of stiffness, the demand to capacity ratios are symmetrically distributed, excepted for the abrupt variation shown at the extremities, such ratios are almost constant.

When the CM is placed in its actual position, the scenario is different because the symmetrical distribution of the ratios D/C is lost. The inelastic demands on the flexible side are greater than those shown on the stiff side. Moving from the stiff to the flexible side, the inelastic demand increases progressively, as shown in Figure 10.

As previously shown (Figure 8), assuming an eccentricity of 6% for the CM, the ratio $\delta_{max}/\delta_{avg}$, obtained by performing an equivalent linear static analysis becomes equal to 1.2. In this configuration, the inelastic demand appears clearly irregular. In approximately 40% of the building (Figure 11), the ratios D/C are almost zero, while in the other part, the inelastic demand increases rapidly moving to the flexible side.

When CM is placed with 14% of eccentricity, the ratio $\delta_{max}/\delta_{avg}$, calculated by an equivalent linear static analysis, is equal to 1.4 (Figure 8). Adopting this configuration, the inelastic response is strongly irregular. As shown in Figure 12, approximately 50% of the building provides no inelastic demand. Conversely, moving to the flexible side, the plastic demand increases rapidly providing high values of the ratio D/C.

In Figure 13, the demand to capacity ratios, calculated by means of nonlinear dynamic analyses, of the three columns on stiff and flexible side (respectively, left columns of frame Y1 and right columns of frame Y2 in Figure 3(b)) are plotted at varying $\delta_{max}/\delta_{avg}$ calculated by the equivalent linear static analysis. In this case, it is worth noting that the inelastic demand is highly dependent on $\delta_{max}/\delta_{avg}$ and that the demand decreases on the stiff side and increases on the flexible side.
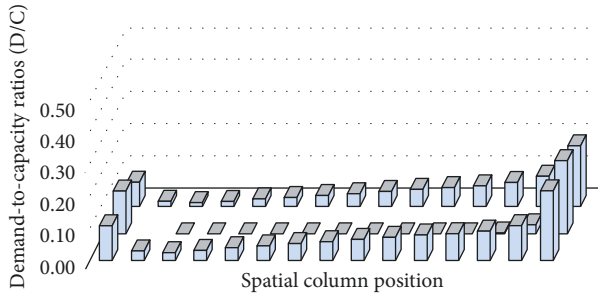
FIGURE 10: Demand to capacity ratios D/C: uneven distribution of inelastic response, CM placed in the actual position.
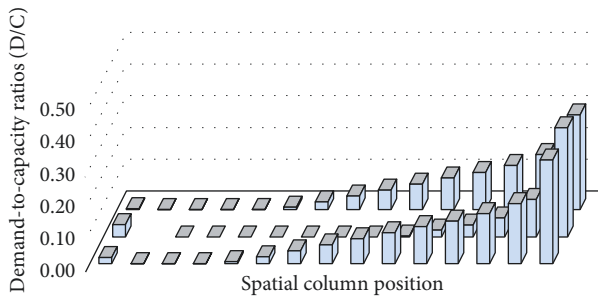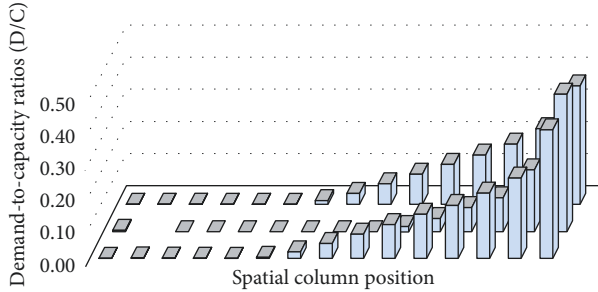

FIGURE 11: Demand to capacity ratios D/C: uneven distribution of inelastic response, CM placed with 6% of eccentricity in order to obtain $\delta_{max}/\delta_{avg} = 1.2$ in the equivalent linear static analysis.

FIGURE 12: Demand to capacity ratios D/C: uneven distribution of inelastic response, CM placed with 14% of eccentricity in order to obtain $\delta_{max}/\delta_{avg} = 1.4$ in the equivalent linear static analysis.
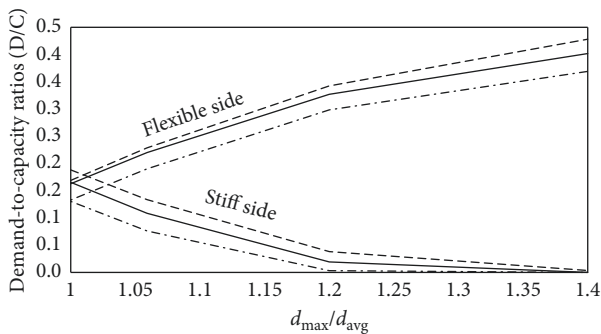

FIGURE 13: Demand to capacity ratios D/C, calculated by means of nonlinear dynamic analyses, at varying $\delta_{max}/\delta_{avg}$ provided by equivalent linear static analysis. Comparison between the inelastic response of the column placed on the stiff side and that provided by the column on the flexible side.

FIGURE 14: Normalized demand to capacity ratios D/C, calculated by means of nonlinear dynamic analyses, at varying $\delta_{max}/\delta_{avg}$ provided by equivalent linear static analysis. Comparison between the inelastic response of the column placed on the stiff side and that provided by the column on the flexible side.
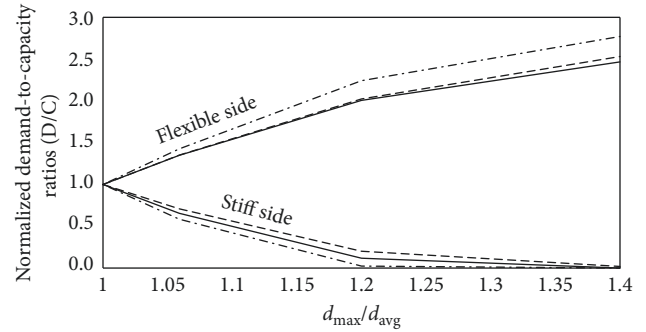
In Figure 14, the demand to capacity ratios are normalized by D/C calculated in configuration CM≡CR, where $\delta_{max}/\delta_{avg}$ is equal to 1. In correspondence of $\delta_{max}/\delta_{avg} = 1.2$, the normalized D/C on the stiff side is about equal to zero, and on the flexible side, it is close to 2.

To investigate the scattering of the damage levels over the building plan, the maximum (D/C)max and average (D/C)avg demand to capacity ratios of all columns at ground floor were computed in the four studied cases (Figures 9–12).

In Figure 15, the inelastic indices $(D/C)_{max}/(D/C)_{avg}$ were normalized by the corresponding $(D/C)_{max}/(D/C)_{avg}$ computed in the configuration in which CM≡CR (i.e., $\delta_{max}/\delta_{avg} = 1$).

Figure 15 clearly shows that the value $\delta_{max}/\delta_{avg} = 1.2$ may be considered as a threshold value beyond which plan scattering of the damage level D/C does not increase significantly. Of course, this result may be affected by the particular condition of the analyzed building, and therefore, it needs to be validated by means of further investigations on different building types.

5. Conclusions

This paper is focused on the evaluation of the ASCE code approach for detecting building plan irregularity. The response of an existing R/C school building, taken as reference case study, is investigated to evaluate how well torsional irregularity detected by the code corresponds to uneven distribution of inelastic demand found by nonlinear dynamic analyses. In particular, for the studied case, the threshold value of 1.2 for identifying buildings plan irregularity seems to be appropriate when plan scattering of damage levels is considered. In this specific case, the value of 1.2 seems already to characterize an extreme torsional irregularity condition, and therefore, the value 1.4 provided by the ASCE code may be too large. However, it is worth noting that this trend could also arise from the specificity of the building under investigation, and therefore, a larger number of existing buildings with different structural arrangements and plan
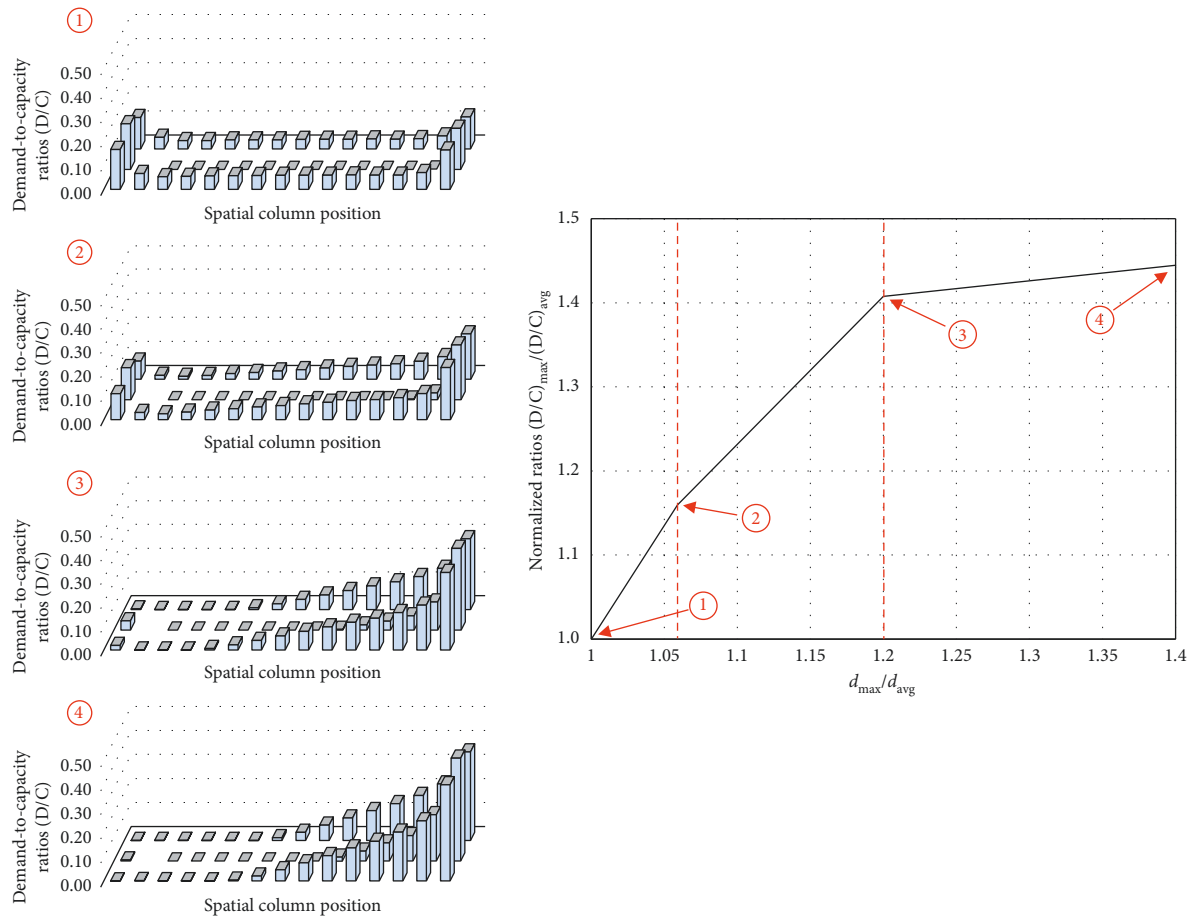
FIGURE 15: Normalized demand to capacity ratios $(D/C)_{max}/(D/C)_{avg}$, calculated by means of nonlinear dynamic analyses, at varying $\delta_{max}/\delta_{avg}$ provided by the equivalent linear static analysis.

configurations are currently under analysis to provide support to this thesis.

Data Availability

The authors state that data in the manuscript are freely available.

Conflicts of Interest

The authors declare that there are no conflicts of interest regarding the publication of this paper.

Acknowledgments

References

[1] M. De Stefano and B. Pintucchi, "A review of research on seismic behaviour of irregular building structures since 2002," *Bulletin of Earthquake Engineering*, vol. 6, no. 2, pp. 285–308, 2007.

[2] E. Rosenlueth and R. Meli, "The 1985 earthquake: causes and effects in Mexico city," *Concrete International*, vol. 8, no. 5, pp. 23–34, 1986.

[3] W. K. Tso, "Static eccentricity concept for torsional moment estimations," *Journal of Structural Engineering*, vol. 116, no. 5, pp. 1199–1212, 1990.

[4] A. M. Chandler and G. L. Hutchinson, "Evaluation of code torsional provisions by a time history approach," *Earthquake Engineering & Structural Dynamics*, vol. 15, no. 4, pp. 491–516, 1987.

[5] A. K. Chopra and R. K. Goel, "Evaluation of torsional provisions in seismic codes," *Journal of Structural Engineering*, vol. 117, no. 12, pp. 3762–3782, 1991.

[6] M. De Stefano, G. Faella, and R. Ramasco, "Inelastic response and design criteria of plan-wise asymmetric systems," *Earthquake Engineering & Structural Dynamics*, vol. 22, no. 3, pp. 245–259, 1993.

[7] C. M. Wong and W. K. Tso, "Evaluation of seismic torsional provisions in uniform building code," *Journal of Structural Engineering*, vol. 121, no. 10, pp. 1436–1442, 1995.

[8] A. M. Chandler, J. C. Correnza, and G. L. Hutchinson, "Influence of accidental eccentricity on inelastic seismic torsional effects in buildings," *Engineering Structures*, vol. 17, no. 3, pp. 167–178, 1995.

[9] M. De Stefano and A. Rutenberg, "A comparison of the present SEAOC/UBC torsional provisions with the old ones," *Engineering Structures*, vol. 19, no. 8, pp. 655–664, 1997.

[10] A. M. Chandler and X. N. Duan, "Performance of asymmetric code-designed buildings for serviceability and ultimate limit states," *Earthquake Engineering & Structural Dynamics*, vol. 26, no. 7, pp. 717–735, 1997.

[11] A. P. Harasimowicz and R. K. Goel, "Seismic code analysis of multi-storey asymmetric buildings," *Earthquake Engineering & Structural Dynamics*, vol. 27, no. 2, pp. 173–185, 1998.

[12] K. Anastassiadis, A. Athanatopoulou, and T. Makarios, "Equivalent static eccentricities in the simplified methods of seismic analysis of buildings," *Earthquake Spectra*, vol. 14, no. 1, pp. 1–34, 1998.

[13] I. Perus and P. Fajfar, "On the inelastic torsional response of single-storey structures under bi-axial excitation," *Earthquake Engineering & Structural Dynamics*, vol. 34, no. 8, pp. 931–941, 2005.

[14] M. De Stefano, M. Tanganelli, and S. Viti, "Effect of the variability in plan of concrete mechanical properties on the seismic response of existing RC framed structures," *Bulletin of Earthquake Engineering*, vol. 11, no. 4, pp. 1049–1060, 2012.

[15] A. Athanatopoulou, G. Manoukas, and A. Throumoulopoulos, "Parametric study of inelastic seismic response of reinforced concrete frame buildings," in *Chapter 15: Geotechnical, Geological and Earthquake Engineering*, vol. 40 of Seismic Behaviour and Design of Irregular and Complex Civil Structures II, Z. Zembaty, M. De Stefano, Eds., pp. 171–180, Springer, Berlin, Germany, 2015, ISBN 978-3-319-14245-6.

[16] R. K. Goel and A. K. Chopra, *Inelastic Seismic Response of One-Story, Asymmetric-Plan Systems*, John Wiley & Sons, Richmond, CA, USA, 1990.

[17] A. D'Ambrisi, M. De Stefano, and M. Tanganelli, "Use of pushover analysis for predicting seismic response of irregular buildings: a case study," *Journal of Earthquake Engineering*, vol. 13, no. 8, pp. 1089–1100, 2009.

[18] G. Magliulo, G. Maddaloni, and E. Cosenza, "Extension of N2 method to plan irregular buildings considering accidental eccentricity," *Soil Dynamics and Earthquake Engineering*, vol. 43, pp. 69–84, 2012.

[19] M. Bosco, A. Ghersi, E. M. Marino, and P. P. Rossi, "Comparison of nonlinear static methods for the assessment of asymmetric buildings," *Bulletin of Earthquake Engineering*, vol. 11, no. 6, pp. 2287–2308, 2013.

[20] G. Manoukas, A. Athanatopoulou, and I. Avramidis, "Multimode pushover analysis for asymmetric buildings under biaxial seismic excitation based on a new concept of the equivalent single degree of freedom system," *Soil Dynamics and Earthquake Engineering*, vol. 38, pp. 88–96, 2012.

[21] P. Fajfar, D. Marusic, and I. Perus, "Torsional effects in the pushover-based seismic analysis of buildings," *Journal of Earthquake Engineering*, vol. 9, no. 6, pp. 831–854, 2005.

[22] C. Bhatt and R. Bento, "The extended adaptive capacity spectrum method for the seismic assessment of plan-asymmetric buildings," *Earthquake Spectra*, vol. 30, no. 2, pp. 683–703, 2014.

[23] S. A. Anagnostopoulos, M. T. Kyrkos, and K. G. Stathopoulos, "Earthquake induced torsion in buildings: critical review and state of the art," *Earthquakes and Structures*, vol. 8, no. 2, pp. 305–377, 2015.

[24] ASCE, *Minimum Design Loads for Buildings and Other Structures, ASCE/SEI 7*, American Society of Civil Engineers, Reston, VA, USA, 2010.

[25] European Committee for Standardization, *Eurocode 8 Design Provisions for Earthquake Resistance of Structures Part 1-2: General Rules—General Rules for Building*, European Committee for Standardization, Brussels, Belgium, 1993.

[26] Associate Committee on the National Building Code, *National Building Code of Canada*, National Research Council, Ottawa, ON, Canada, 1995.

[27] European Committee for Standardization, *Eurocode 8 Design of Structures for Earthquake Resistance—Part 1: General Rules, Seismic Actions and Rules for Buildings Eurocode*, European Committee for Standardization, Brussels, Belgium, 2004.

[28] Associate Committee on the National Building Code, *National Building Code of Canada*, National Research Council, Ottawa, ON, Canada, 2010.

[29] SAP2000, CSI, *Integrated Software for Structural Analysis & Design*, Computer and Structures, Inc., Berkeley, CA, USA, 2007.

[30] DM.LL.PP.2018, 17 Gennaio 2018, Norme Tecniche Per Le Costruzioni (NTC), G.U. n. 42 del 20 febbraio 2018.

[31] F. Pugi and S. Galassi, "Seismic analysis of masonry voussoir arches according to the Italian building code," *International Journal of Earthquake and Impact Engineering*, vol. 30, no. 3, pp. 33–55, Patron, Bologna, Italy, 2013.

[32] ASCE, *Seismic Evaluation and Retrofit of Existing Buildings (ASCE 41-13), ASCE/SEI 4*, American Society of Civil Engineers, Reston, VA, USA, 2014.